The Performance and Design Checking of Chord-Angle Legs in Joist Girders

THEODORE V. GALAMBOS

ABSTRACT

The subject of this paper is the development of a design checking method for the capacity of the outstanding legs of the compression chord in joist girders subjected to eccentric reaction forces from the bearing seats of the joists bearing on these chords at panel points. Fifteen tests were performed, and, based on these tests and on plastic analysis, a conservative formula for the ultimate strength of the outstanding legs has been developed. A design checking formula is also proposed.

INTRODUCTION

Joist girders are standard trusses designed in accordance with the Steel Joist Institute *Standard Specification for Joist Girders* (SJI, 1994) to act as primary load-carrying beam elements in a structural frame. Secondary members, usually standard open-web steel joists, bear at the girder panel points on the outstanding legs of the top chord angles. This report describes the results of tests and analyses conducted to determine the capacity of these outstanding legs to support the end-bearing seat of the joist. Simple elastic analysis, modeling the outstanding angle leg as a cantilever, indicated that the chord angle leg alone, without local reinforcement, could not carry the joist reactions. Yet no distress or failure has been observed in practice, where no such reinforcement is usually provided. A more realistic method of analysis is therefore needed. The tests and analyses reported herein, as well as the results of research on the strength of wide-flange beam tension flanges subjected to concentrated hanging loads (Dranger, 1977; Gobetti and Zanon, 1980; and Ballio, Poggi, and Zanon, 1981), showed that eventually a plastic mechanism forms, and that, upon further deformation, also develops a tension field. Due to this reserve in strength the joist girder chords are usually able to support the joist reactions they are called upon to carry, without a need for reinforcement. The research reported herein is performed to provide a method for the joist girder manufacturers to check the chords.

DESCRIPTION OF THE TESTS

The details of the joist girder and joist bearing seat assembly are shown in Figure 1. Two types of tests were performed: using a truss assembly and a beam-type assembly. Figure 2 shows a truss assembly where the bottom chord was placed directly on the base of the testing machine, and the top chord was loaded eccentrically through two end-bearing seat stubs (Figure 3). No axial stress along the longitudinal axis of the compression (top) chord was present in this experimental setup. Further tests were made on a beam-type assembly (Figures 4 and 5) that was made from four angles welded into an I-shaped cross section. In this type of test, both transverse bending and longitudinal axial stress were present in the outstanding chord leg. These latter tests

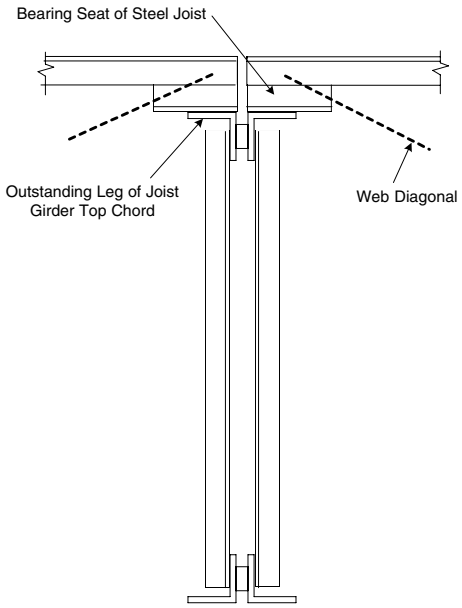

Fig. 1. Joist bearing on joist girder at panel point.

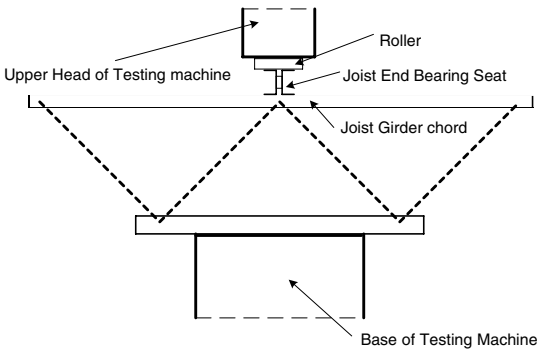

Fig. 2. Test specimen details for tests 1 through 7.

Theodore V. Galambos is emeritus professor of structural engineering, University of Minnesota, Minneapolis, MN.

thus simulate the actual conditions far better than the first tests.

Each type of test was performed by applying load from a hydraulic testing machine by rollers to the joist end-bearing seat stub, and thus to the outstanding leg of the joist girder chord. Transverse bending to this outstanding leg resulted from the couple Pe^*, where P is one-half the load recorded on the testing machine load indicator and e^* is the distance between the line of action of P and the toe of the inside fillet of the chord angle (see Figure 3). The definition of the line of action assumes a uniform distribution of the force over the area of contact. This is a somewhat arbitrary simplification of reality, because there is no perfect contact between the two surfaces. In addition to the load data, the total downward deflection of the top chord and the deflections of the toes of the chord angles or the tips of the bearing stubs were recorded. Loading was continued until the outstanding legs of the chords were extensively yielded and grossly deformed, i.e., well beyond the formation of the yield mechanism and into the range where tension field (catenary membrane) action was observed.

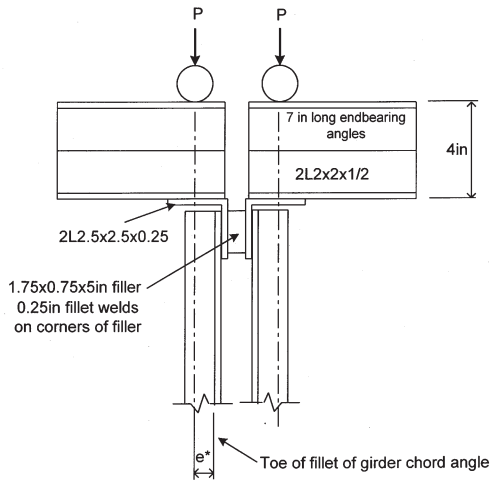

Fig. 3. Loading arrangement for tests 1 through 7.

A drawing of a typical yield mechanism is shown in Figure 6. The outstanding leg of the girder chord angle deformed as a rotating rigid plate under the surface area of the part of the bearing seat covering it, forming yield lines longitudinally over width g along the toe of the inside fillet of the chord angle and transversely along both edges of the seat. The dimension g is the width of the joist bearing seat and $g = 5$ in. in all tests. Two diagonal yield lines extending away from the bearing area completed the mechanism. After the full development of the plastic mechanism, longitudinal tension field yield lines could be observed in the triangular zones as the load continued to rise. The photograph in Figure 7 shows a typical yield line pattern characterized by the dark lines on the whitewashed chord. The outlines of the plastic mechanism, shown in idealized form in Figure 6, can be discerned in the photograph.

The pertinent details of the test series are given in Tables 1 and 2. These data consist of the material properties as obtained from tensile coupon tests of the chord steel; the chord angle sizes; the measured thickness of the angle legs; the eccentricities e^* (see Figures 5 and 6); and the load P_u^{test} (see Figures 3 and 5) when loading was discontinued because of excessive deflection of the angle leg.

Typical load-versus deflection plots are presented in Figures 8 through 10. The load P is the force acting on one-half of the joist girder chord (see Figures 3 and 5), and the deflection is the relative downward displacement of the end of the joist bearing stub (7 in. from the center of the joist girder chord) with respect to the deflection of the center. The experimental curves in Figures 8 and 10 characterize the effect of the eccentricity of the load, indicating the influence of this variable. The curves in Figure 9 show the behavior of two identical specimens tested with essentially the same eccentricity. One specimen, (B2-1) was tested as a beam (see Figure 4), while the other one (B2-2) was tested with the bottom flange of the beam placed flat on the base of the testing machine. The first test specimen was subjected, therefore, to both transverse bending from the

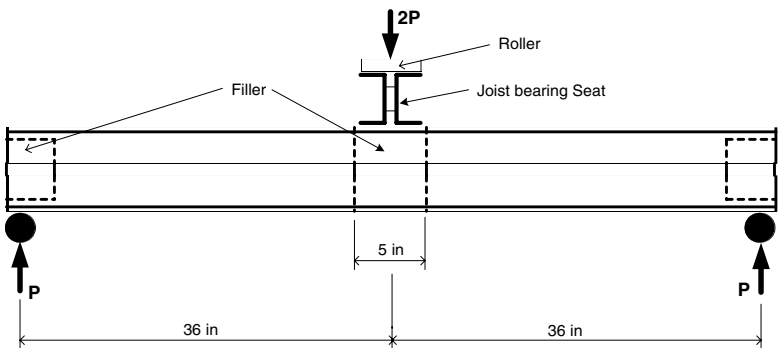

Fig. 4. Test specimen details for tests B1 through B4.

Table 1. Summary of Tests 1 through 7 (Figs. 2 and 3).

Joist girder chord angle sizes: 2 ½ x 2 ½ x ¼
Measured thickness of angle leg: 0.235 in.
Yield stress of steel: 66.6 ksi
Tensile strength of steel: 99.1 ksi

Test Number [c]	e^* (in.)	P_u^{test} (kips)	P_p (kips)	P_u^{test}/P_p	Length of ¼ in. weld on filler
1	0.69	23.9	21.3	1.12	4
2	1.94	10.0	7.6	1.32	4
3	1.32	13.3	11.2	1.19	4
4	0.69	35.0	21.3	1.69	2
5	2.94	5.65	5.0	1.13	4
6 [a]	1.94	7.8	7.6	1.03	4
7 [b]	0.69	17.8	21.3	0.84	4

[a] ⅛ in. cover plate between top of chord and bearing.

[b] Retest of Test 3, loaded on side that was previously least deformed.

[c] No longitudinal axial stress.

Table 2. Summary of Tests B1 through B4 (Figs. 4 and 5).

Test	Chord Size	t (in.)	F_y (ksi)	F_u (ksi)	e^*	P_p (kips)	P_y (kips)	P_u^{test} (kips)	P_u^{test}/P_p	P_u^{test}/P_y
B1-1	3 x 3 x ¼	0.254	51.3	80.7	0.92	16.9	18.1	16.3	0.964	0.901
B1-2	3 x 3 x ¼	0.253	51.8	82.3	2.45	6.4	18.3	10.4	1.625	0.568
B2-1	3 ½ x 3 ½ x 5⁄16	0.322	48.8	74.7	1.05	25.2	28.6	25.0	0.992	0.874
B2-2 [a]	3 ½ x 3 ½ x 5⁄16	0.322	48.8	74.7	1.00	26.4	—	46.6	1.761	0
B3-1	4 x 4 x ⅜	0.375	51.8	81.3	1.31	32.5	46.6	37.5	1.154	0.805
B3-2	4 x 4 x ⅜	0.375	51.8	81.3	3.25	13.1	46.6	16.2	1.237	0.348
B4-1	4 x 4 x ½	0.504	45.9	75.9	1.16	57.0	52.7	46.5	0.816	0.882
B4-2 [a]	4 x 4 x ½	0.504	45.9	75.9	1.12	59.0	—	67.5	1.144	0

[a] Tested with base of beam flat on platen of testing machine: no longitudinal stresses.

eccentric load and longitudinal stress due to beam flexure, while the second test specimen was only under transverse bending. A comparison of the curves in Figure 9 show the significant influence of the longitudinal compressive force in reducing the strength of the outstanding legs of the compression chord of the joist girder.

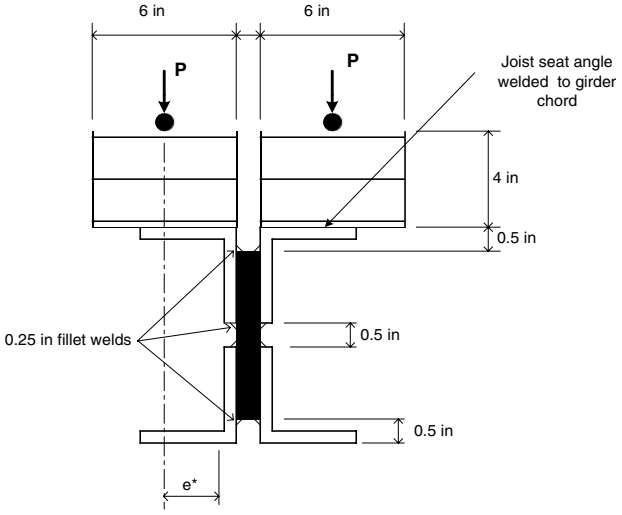

Fig. 5. Loading arrangement for tests B1 through B4.

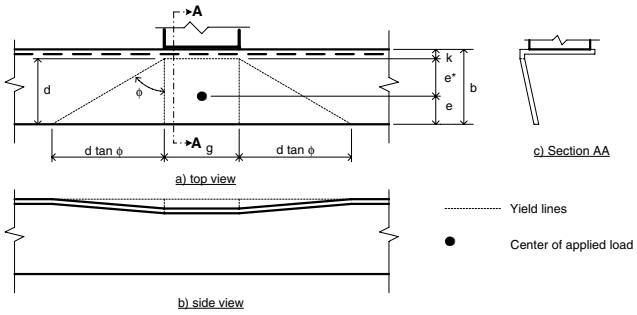

Fig. 6. Geometry of the plastic mechanism.

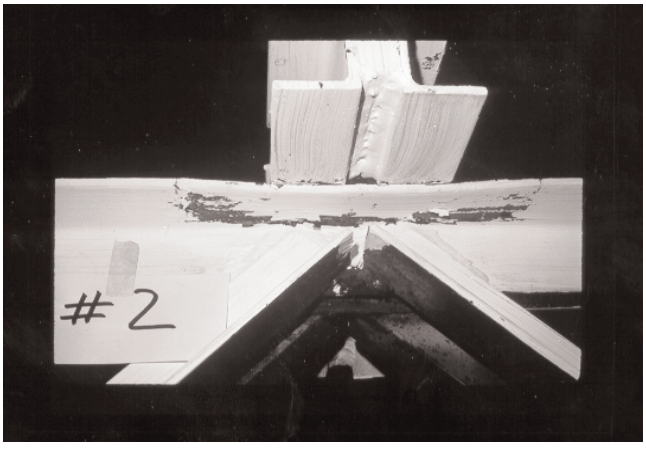

Fig.7. Plastic mechanism seen on test specimen.

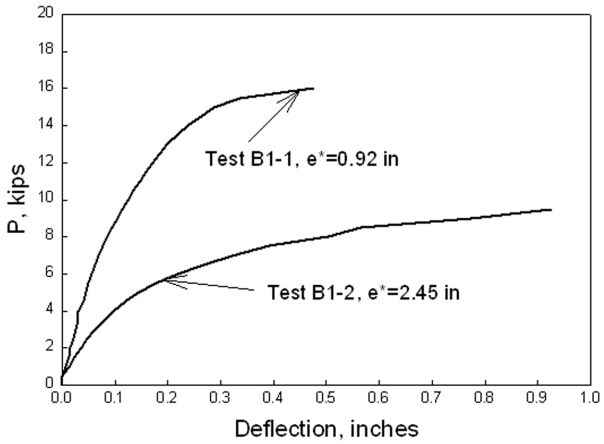

Fig. 8. Load vs. bearing-stub-end deflection for tests B1-1 and B1-2.

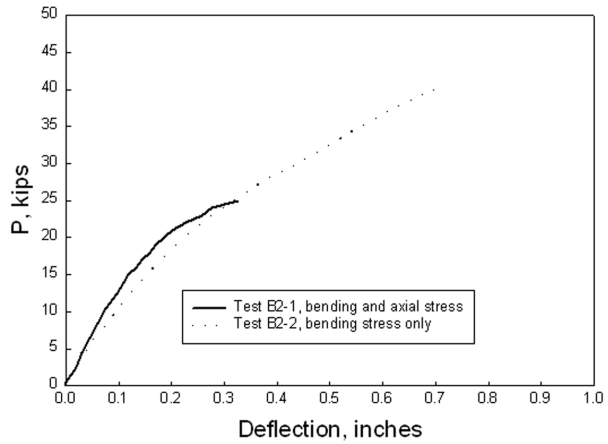

Fig. 9. Load-deflection curves for tests B2-1 and B2-2.

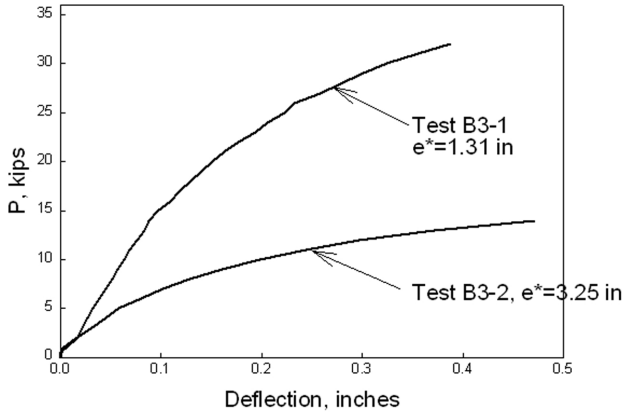

Fig. 10. Load-deflection curves for tests B3-1 and B3-2.

THEORETICAL ANALYSIS

The first series of tests (Tests 1 through 7, Table 1) were experiments where only transverse bending due to the eccentrically applied force to the outstanding leg was present. The deformation behavior clearly indicated a pattern suggesting a plastic plate mechanism, and thus an analysis of such a mechanism is appropriate. Such an analysis was used in Dranger (1977) for a similar problem. The plastic analysis derivation is given in the Appendix. The resulting plate mechanism collapse load P_p is:

$$P_p = (M_p/e^*)(g + 5.66d) \quad (1)$$

where

g = width of bearing seat (g = 5 in. in all tests)

d = distance between the toe of the outstanding chord angle leg and the toe of the inside of the fillet

M_p = plastic moment of a one-inch width of the outstanding angle leg,

$$M_p = t^2F_y/4 \quad (2)$$

The computed plastic collapse load P_p is the predicted ultimate capacity for the tests that were subjected to only transverse bending (Tests 1 through 7 in Table 1 and Tests B2-2 and B4-2 in Table 2). The ratios of the experimental to the predicted ultimate loads are, with the exception of Test 7, above unity, with the average ratio for the nine tests being 1.25. Test 7 was a retest with load applied only on one side of a previously tested specimen. Thus the low ratio of 0.84 is not surprising. One reason for the conservative prediction of the ultimate strength is that the analysis did not account for the tension field action that developed with large deformations of the plate.

The prediction of the ultimate strength of the test specimens that were subjected to both transverse and longitudinal bending is based on the empirical interaction lines shown in Figure 11. The interaction limits are three straight lines. All the test points fall above these lines, with exception of Test 7. The interaction lines are defined by the following three equations:

$$\begin{aligned} &\frac{P_u}{P_y} + \frac{P_u}{P_p} \le 1.6 \\ &P_u \le P_y \\ &P_u \le P_p \end{aligned} \quad (3)$$

where

P_u = Predicted ultimate capacity

P_p = Plastic mechanism collapse load

P_y = Load to produce flexural yielding in the joist girder chord

For the present tests P_y is the load that would be required to yield the compression chord of the test beam in the absence of transverse eccentricity. Since the center of the beam is reinforced by a one-inch thick filler plate (Figures 4 and 5), the critical section is just outside the end of the filler plate, 36 − 2.5 = 33.5 in. from the end support of the beam (Figure 4). Thus

$$M = 33.5P_y = S_xF_y \quad (4)$$

where

F_y = Yield stress, ksi

S_x = Elastic Section Modulus of the four-angle beam cross section (Figure 5, not counting the filler plate), in.^{3}

The yield force P_y is, therefore, defined by the equation

$$P_y = S_xF_y/33.5 \quad (5)$$

The values of P_y, as well as P_p from Equation 1 and the ratios P_u^{test}/P_y and P_u^{test}/P_p are tabulated in Table 2 for the appropriate tests (B1-1, B1-2, B2-1, B3-2 and B4-1). All of the test-to-prediction ratios are shown in the interaction space in Figure 11. It is evident that the interaction equations (Equations 3) are conservative lower bound predictions for all tests except Test 7. The main cause for this conservatism is, again the fact that tension field action was not included in the analysis while the test behavior clearly indicated the presence of this effect.

DESIGN CHECKING RECOMMENDATION

A conservative recommendation for a design checking method is based on the scaling down of the interaction lines shown in Figure 11 to an allowable value of the joist end-reaction with a theoretical factor of safety of 1/0.6 = 1.67 against failure of the joist girder top chord under a concentrated load. This design interaction surface is shown in Figure 12. The ordinate of the coordinates is the joist reaction divided by $0.6P_p$, where P_p is the plastic failure load of the outstanding leg in the absence of a longitudinal stress, defined by Equation 1. The abscissa is the ratio $f_a/0.6QF_y$, where f_a is the axial stress in the joist girder top chord and Q is the form factor defined in SJI (1994). The interaction equation shown in Figure 12 can be rearranged into the following design checking format:

$$R \le 0.6P_p\left[1.6 - \frac{f_a}{0.6QF_y}\right] \le 0.6P_p \quad (6)$$

The allowable design panel point load on the joist girder is twice the allowable reaction. The reaction is assumed to act at the center of the distance between the toe of the out-

standing chord angle leg and the toe of the inside fillet of the angle. Thus $d = b - K$ and $e^* = (b - K)/2$, where b is the width of the outstanding angle leg and K is the distance between the outside edge of the angle and the toe of the fillet. The value of K is obtained from a handbook of angle properties. The equation of P_p can now be written as:

$$P_p = \frac{t^2 F_y}{2(b-K)}\left[g + 5.66(b-K)\right] \qquad (7)$$

The following example illustrates the application of the proposed design checking procedure:

Joist girder designation: 36G6N20.5K
Panel point load: P = 20.5 kips
Chord angle size: 2L4×4×⅜
t = 0.375 in.
b = 4.0 in.
K = 0.75 in.
Q = 1.0
F_y = 50 ksi
g = 5.0 in.
From structural analysis: f_a = 27.11 ksi

$$P_p = \frac{t^2 F_y}{2(b-K)}\left[g + 5.66(b-K)\right]$$
$$= \frac{0.375^2 \times 50}{2\times(4-0.75)} \times \left[5 + 5.66 \times (4-0.75)\right]$$
$$= 25.31 \text{ kips}$$

Allowable reaction:

$$R_a = \min\left[0.6P_p, 0.6P_p\left(1.6 - \frac{f_a}{0.6QF_y}\right)\right]$$
$$= \min\left[0.6\times 25.31, 0.6\times 25.31 \times \left(1.6 - \frac{27.11}{0.6\times 1.0\times 50}\right)\right]$$
$$= \min\left[15.18, 10.57\right] = 10.57 \text{ kips}$$

The allowable panel point load is then $2R_a = 2 \times 10.57 = 21.14$ kips > 20.5 kips **OK**.

CONCLUSION

The tests on the strength of the outstanding legs of the compression chords of joist girders that support the reactions from the bearing seats of joists demonstrated that failure was due to the formation of a plastic plate mechanism in the outstanding angle leg. Load carrying capacity was enhanced by the development of a tension field in the outstanding angle leg that forms even in the presence of longitudinal compressive stress. The final failure of the specimen was due to excessive deformation that was far greater than the tolerable end-rotation of the joist end. A conservative design checking equation is recommended for use in the design of joist girders (Equation 6). This checking method is strictly applicable only to joists bearing on joist girders. Extrapolation to other details should be done with caution.

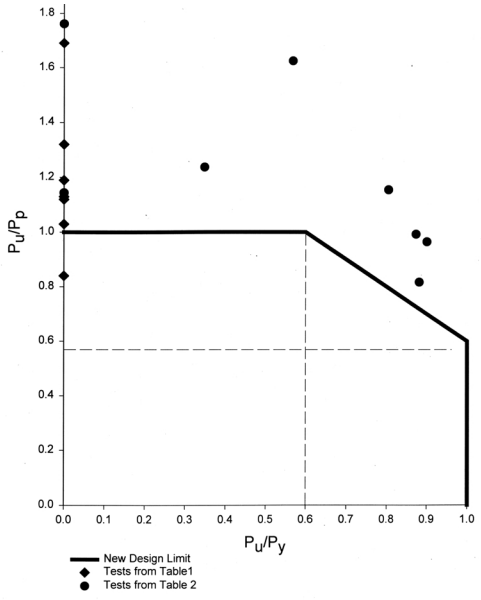

Fig. 11. Test results on the interaction space.

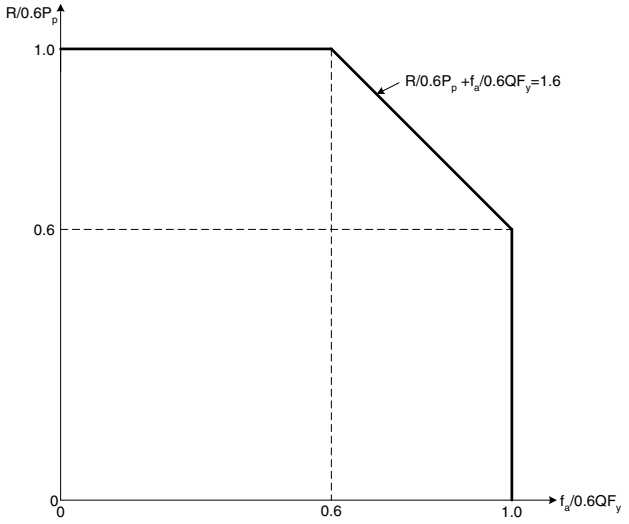

Fig. 12. Design interaction space.

ACKNOWLEDGMENTS

The Steel Joist Institute sponsored this research and the SJI Research Committee, of which Mr. Wayne Studebaker is the chairman, supervised it. The testing was performed in the structural engineering laboratory of Washington University in St. Louis during the summers of 1980 and 1981. The assistance of Mr. Lee Edelmann, formerly a student at Washington University, is gratefully acknowledged. Many thanks are due to the members of the SJI Research Committee, especially to Messrs. Studebaker and Potts, who provided data and motivation to reopen this research project 18 years after the first report was written.

NOMENCLATURE

b = width of angle leg
d = flat width of angle leg
e^* = eccentricity of bearing reaction
F_u = tensile strength
F_y = yield stress
f_a = axial compressive stress in chord of joist girder
g = width of bearing seat
K = angle depth minus flat width
M_p = plastic moment per unit length
P = concentrated load
P_p = force causing plastic mechanism
P_y = yield load
Q = form factor
R = reaction of joist
S_x = elastic section modulus
t = thickness of angle leg

REFERENCES

Steel Joist Institute (SJI) (1994), *Standard Specification for Joist Girders*, Myrtle Beach, SC.

Dranger, T.S. (1977), "Yield Line Analysis of Bolted Hanging Connections", *Engineering Journal*, American Institute of Steel Construction, 3rd Quarter, Vol. 14, No. 3, Chicago, IL.

Gobetti, A. and Zanon, P. (1980), "Influence of the Membrane Effects of the Collapse Behavior of Bending Plates Subject to Concentrated Loads," *Costruzioni Metalliche*, No. 4, Milano, Italy (in English).

Ballio, G., Poggi, C., and Zanon, P. (1981), "Notes on the behavior of Crane Girder When Loads are Concentrated on the Lower Flange," *Costruzioni Metalliche*, No. 1, Milano, Italy (in English).

APPENDIX:
DERIVATION OF PLASTIC COLLAPSE LOAD

A kinematic mechanism of one-half of the top chord (i.e., one of the angles) of the joist girder is shown in Figure A. The force P due to the joist bearing seat reaction on this half-top chord performs the external work (Figure A) due to the virtual rotation θ of the yield line that is parallel to the top chord axis along the line formed by the toe of the fillet of the angle.

$$W_e = P\theta e^* \tag{A-1}$$

The internal virtual work is the product of M_p, the plastic moment per unit length of the angle leg plate, and the rotation between the intersecting plate segments along the yield lines:

$$W_i = M_p\theta g + \frac{2M_p\theta d}{\tan\phi} + \frac{2d}{\cos\phi}\times\frac{M_p\theta}{\sin\phi} \tag{A-2}$$

The first term is due to the rotation of the yield line at the end of the fillet (Figure A(c)), the second one is due to the rotation of the vertical yield lines (Figures A(a) and A(d)), and the last term is due to the rotation of the diagonal yield lines (Figures A(a), A(b) and A(d)).

By setting $W_e = W_i$, the plastic collapse load is obtained, i.e.,

$$P_p = \frac{M_p}{e^*}\left\{g + \frac{2d\left(\cos^2\phi + 1\right)}{\sin\phi\cos\phi}\right\} \tag{A-3}$$

The angle φ is determined by noting that the correct plastic collapse mechanism is the smallest possible P_p obtained from Equation A-3, i.e.,

$$\frac{\partial P_p}{\partial\varphi} = 0$$

$$= \frac{\left(-2\cos\phi\sin\phi\right)\left(\sin\phi\cos\phi\right) - \left(\cos^2\phi + 1\right)\left(\cos^2\phi - \sin^2\phi\right)}{\left(\sin\phi\cos\phi\right)^2}$$

from which $\cos\phi = \frac{1}{\sqrt{3}}$ and φ = 54.7°.

Substitution of φ into Equation A-3 gives the equation for the plastic collapse load:

$$P_p = \frac{M_p}{e^*}\left[g + 5.66d\right] \tag{A-4}$$

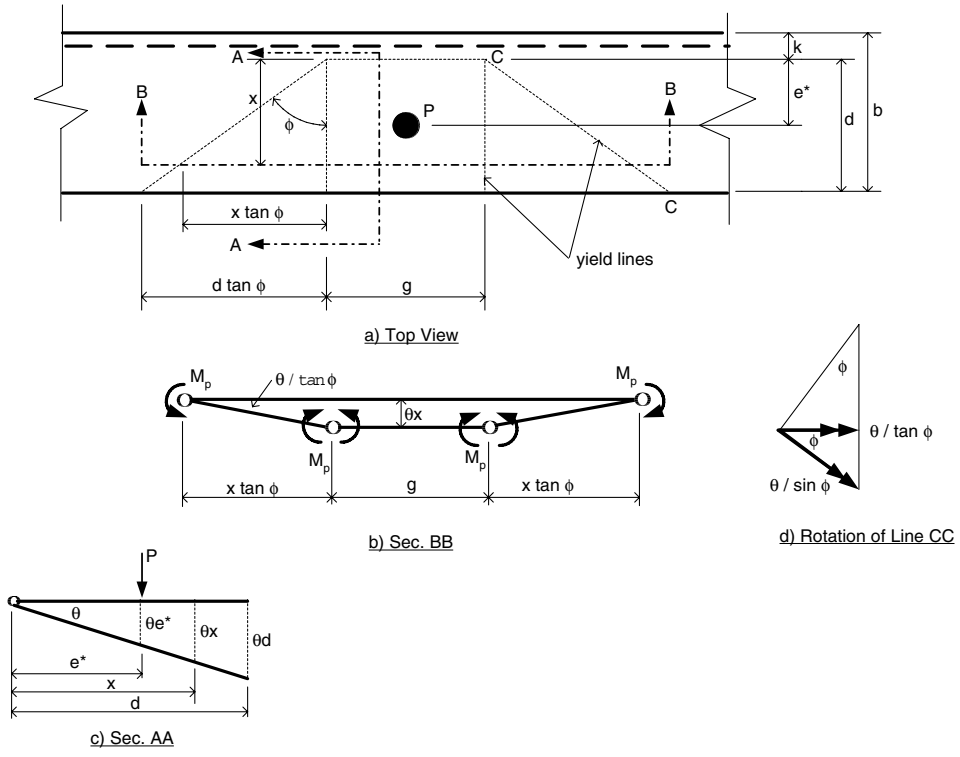

Fig. A. Plastic mechanism geometry.